

**HEAT FLUX MICROSENSOR MEASUREMENTS AND CALIBRATIONS**

James P. Terrell and Jon M. Hager  
Vatell Corporation  
Blacksburg, VA

Shinzo Onishi and Thomas E. Diller  
Virginia Tech  
Blacksburg, VA

**SUMMARY**

A new thin-film heat flux gage has been fabricated specifically for severe high temperature operation using platinum and platinum-10% rhodium for the thermocouple elements. Radiation calibrations of this gage were performed at the AEDC facility over the available heat flux range ( $\sim 1.0 - 1,000 \text{ W/cm}^2$ ). The gage output was linear with heat flux with a slight increase in sensitivity with increasing surface temperature.

Survivability of gages was demonstrated in quench tests from  $500^\circ\text{C}$  into liquid nitrogen. Successful operation of gages to surface temperatures of  $750^\circ\text{C}$  has been achieved. No additional cooling of the gages is required because the gages are always at the same temperature as the substrate material. A video of oxyacetylene flame tests with real-time heat flux and temperature output is available.

**INTRODUCTION**

The measurement of high heat flux is a primary concern for the aerospace industry. Existing heat flux sensors lack the reliability and durability needed for use in high temperature, high heat flux environments. These applications include gas turbine blades, hypersonic combustion chambers, rocket nozzles, and atmospheric reentry panels. Harsh environments such as these can produce wall temperatures in excess of  $3,000^\circ\text{C}$ , heat fluxes of more than  $2,000 \text{ W/cm}^2$  and flow speeds reaching Mach 25. These environments may also possess rapid transient processes which require a sensor with fast time response ( $< 1 \text{ msec}$ ).

There are some existing heat flux sensors that have been used for aerospace applications [1]. The high temperature Gardon gages can survive temperatures up to 1000°C and have a time response of 0.2 to 5.0 seconds [2]. Because most Gardon gages have a temperature limit of 500°C, they must be water cooled. Schmidt-Boelter gages normally survive temperatures to 350°C and have a time response  $\geq 0.05$  seconds [3]. Null-point calorimeters are designed for high heat flux measurements ( $> 100 \text{ W/cm}^2$ ) and run times less than 0.5 sec [4]. Heat flux can also be inferred from surface temperature measurements and the substrate thermal properties. Because the measurement depends upon a change in temperature with time, however, the flow conditions must be rapidly changed or the model must be injected into the flow. Jones [5] discusses the required signal processing to extract heat flux from the signal. Temperature measurements using coaxial thermocouples, thin-film resistance elements, and temperature sensitive paints have all been used with some success in impulse facilities. Any one of these gages can only partially satisfy the necessary requirements of the high temperature, high heat flux environments described above.

Heat flux gages often cause the problems of flow field and temperature field distortion. This is especially true for high speed flow and high temperature applications. Flow field distortion can be minimized by fairing the gage surface with its surroundings. In contrast, a distortion free temperature field is difficult to maintain in the presence of a heat flux gage. The distortion is due mainly to the discontinuity of material thermal properties when the flow encounters the gage. For high temperature applications, heat flux gages are often actively cooled to prevent overheating, which creates a cold spot. This will obviously magnify the thermal disruption and alter the heat flux measured. This is a problem with many of the previous measurements in these environments [6].

Layered heat flux gages, as illustrated in Fig. 1, have recently been made with thin film techniques, as first reported by Hager et al. [7]. Called Heat Flux Microsensors, they consist of several thin-film layers forming a differential thermopile across a thermal resistance layer. Because the gages are sputtered directly onto the surface, their total thickness is less than  $2 \mu\text{m}$ , which is much less than previous layered gages. The resulting temperature difference across the thermal resistance layer ( $\delta < 1 \mu\text{m}$ ) is very small even at high heat fluxes. To generate a measurable signal many thermocouple pairs are put in series, as illustrated in Fig. 2. The combination of series thermocouple junctions and thin-film design creates a gage with very attractive characteristics for aerodynamic measurements. It is not only physically non-intrusive to the flow, but also causes minimal disruption of the surface temperature. Because it is so thin, the response time, as reported by Hager et al. [8], is approximately  $20 \mu\text{sec}$ . Unlike the transient thin-film gages, however, the signal of the Heat Flux Microsensor is proportional to the heat flux and gives a continuous measurement. Therefore, it can be used in both steady and transient flows and measures both the steady and unsteady components of the surface heat flux.

A new version of the Heat Flux Microsensor has been developed that has approached meeting the extreme demands exhibited by high temperature, high heat flux environments. These gages use platinum and platinum-10% rhodium as the thermoelectric materials. The melting temperature for platinum is 1700°C and for rhodium, 1900°C. A protective coating of  $\text{Al}_2\text{O}_3$  is

deposited on top of the sensor. The through connection method reported by Hager et al. [9] has survived saturation temperatures to 1000°C. This paper describes the radiation calibrations of these gages at the Arnold Engineering Development Center facility and experimental tests with an oxyacetylene flame and a liquid nitrogen quench.

## MICROSENSOR FABRICATION

Heat Flux. Microsensors are fabricated with a thin thermal resistance layer ( $< 1 \mu\text{m}$ ) placed between many thermocouple pairs to create a differential thermopile. The individual voltage outputs of each thermocouple pair are too small to measure, however, many pairs arranged in series elevate the signal to a measurable level. The output voltage of the thermopile is directly proportional to the temperature difference across the thermal resistance layer, which is proportional to the heat flux normal to the surface.

The microsensors are made using thin-film sputtering techniques with stainless steel masks. A separate mask is made for each different layer by cutting with a programmable laser and is aligned one at a time under a microscope until all six layers of the sensor have been completed. Since using the stainless steel masks doesn't require any substrate chemical processing, such as photoresist, the deposition temperature can be increased to 300-400°C. Raising the substrate temperature during deposition reduces the thermal stresses in the film and gives better adhesion of the thin film layers at elevated temperatures. An overlay of the entire pattern is shown in Fig. 3. The surface temperature of the gage is monitored with a platinum thin-film resistance temperature sensor (RTS) located next to the heat flux gage.

A through connection technique has been developed to bring the sensor signal from the material surface through the substrate [9]. This method requires a pin to be inserted after the microsensor is fabricated. The top of the pin is conical in shape to increase the contact area with the hole in the substrate. Matching conical holes are drilled in the substrate before deposition, allowing the metal films to be sputtered down into the holes. Electrical connection between the pin and the film is achieved by compressive contact of the two surfaces. The compressive force is exerted by a miniature push nut encircling the shank of the pin and pressing against the backside of the substrate. A thin protective layer of  $\text{Al}_2\text{O}_3$  is deposited over the gage and the pins for abrasive and chemical protection as well as electrical isolation from the environment. This through connection method has proven to be reliable to over 1000°C. Platinum lead wires are spot welded to the other end of the pins and then connected to their respective twisted pair as part of a four-lead shielded cable.

These gages contribute negligible flow disruption since they are less than  $2 \mu\text{m}$  total thickness. The microsensor fabrication method offers the possibility of preparing a gage directly on the measurement surface or on a plug of the same material. The current gages were deposited on 6.3 mm (0.25 in.) thick, 25.4 mm (1.0 in.) diameter aluminum nitride disks. When gages are deposited on the actual model to be used, or at least the same material, gage thermal disruption

could be virtually eliminated. The small thickness of the gage contributes negligible thermal capacity and affords a high frequency response allowing measurements up to 50 kHz [7].

## MICROSENSOR CALIBRATION

The precision of a heat flux gage measurement is largely based upon the reliability of the calibration. Due to the dependence on independent parameters, such as temperature, it is important to calibrate a gage at or near test conditions. For future success of the Heat Flux Microsensor in extreme environments, there must be a calibration method simulating these high temperature, high heat flux environments. Presently there are very few facilities which can simulate these conditions.

The present gage was calibrated at the AEDC radiation facility, which has the capability to calibrate sensors with heat flux spanning three orders of magnitude. Two of their calibration devices were used for these tests, one for low heat flux (1.0 - 9.1 W/cm<sup>2</sup>) and one for high heat flux (200 - 685 W/cm<sup>2</sup>). Each heat flux range utilized a separate apparatus. The low range calibration method is traceable to NIST [10]. The higher range used a Gardon gage, calibrated by Medtherm, for the standard.

The low heat flux apparatus uses a bank of nine 1,000 watt quartz tube lamps to radiate down through a shutter system. An area of approximately 2.5 cm (1 in.) by 7.5 cm (3 in.) receives radiation uniform to within 1.0%. The gage was mounted in a horizontal aluminum plate along with three Schmidt-Boelter gages used as standards. Because portions of the Heat Flux Microsensor are transparent, the sensors were coated with Krylon Ultra-flat black paint with an emissivity of 0.97. The shutter system allows the lamp bank to preheat to full intensity before the gages are exposed. A single test lasts 10 seconds with data recorded every 0.1 seconds. The data acquisition system was controlled by a microcomputer. A program presented the voltage output of the three standards, their corresponding heat fluxes, and the calculated sensitivity of the Heat Flux Microsensor based on the average heat flux of the three standards. The level of incident heat flux was changed by adjusting the voltage supply to the lamp bank. Several settings were retested to check the repeatability of the tests. The sensitivity of the gage is plotted versus heat flux (Fig. 4) and surface temperature (Fig. 5). The average sensitivity was calculated to be 1.65  $\mu\text{V}/(\text{W}/\text{cm}^2)$  with a standard deviation of 0.13  $\mu\text{V}/(\text{W}/\text{cm}^2)$ .

The high heat flux apparatus radiated upwards using a 1.6 kW Xenon arc lamp focused through a series of shutters. The lamp was capable of producing 2.8 kW/cm<sup>2</sup>. After the radiation passed through the shutter system it was directed through an optical integrator to assure a uniform intensity over the 0.63 cm (0.25 in.) diameter area covering the gage. Unfortunately, the integrator reduced the radiation flux to a maximum level of approximately 700 W/cm<sup>2</sup>. The shutter system consisted of three separate shutters all of which were computer actuated. The shutter system provided radiation protection and allowed evaluation of gage time response. The incident heat flux could be controlled by adjusting the supply voltage to the arc lamp. The small

area of the optical integrator ( $\approx 32 \text{ mm}^2$ ,  $0.05 \text{ in}^2$ ) allowed only one gage to be irradiated at a time. The Gardon gage was placed in the apparatus first to determine the flux level for a 500 msec test. It was then replaced with the microsensor and irradiated with the same voltage setting. The sensitivity of the gage was calculated using the heat flux measured by the Gardon gage,  $q_r$ , the emissivity of the paint on the microsensor,  $\epsilon$ , and the microsensor voltage output,  $q_m$ .

$$S = \left( \frac{1}{\epsilon} \right) \left[ \frac{E_m}{q_r} \right] \quad (1)$$

The resulting gage sensitivities are plotted versus gage surface temperature for four different heat flux levels in figure 6. Because of the high heat flux levels, the surface temperature of the gage rose noticeably even over the short 50 msec time of each test. The temperature dependence of sensitivity is evident over this temperature range. The average sensitivity increase of  $0.44\%/^{\circ}\text{C}$  may be explained by the decrease in thermal conductivity of the thin thermal resistance layer with increasing temperature. When compared with the low heat flux calibrations, the sensitivity at high heat flux is about 20% lower at the same surface temperature. Although this is not a large difference considering the range of almost three orders of magnitude in heat flux, there are several uncertainties in the high heat flux calibrator results. First, the manufacturer's calibration of the Gardon gage standard had to be used because a standard from NIST was not available. Second, the effect of elevated temperatures on the Gardon gage is not known. Third, the emissivity of the paint was assumed to remain constant at 0.97, although its surface finish was noticeably altered after the high heat flux calibrations. Fourth, the spot size of the calibrator was barely larger than the 3 mm by 4 mm size of the microsensor.

Aerodynamic applications for heat flux sensors involve placing the sensor in a flow field. Although the primary mode of heat transfer is often convection, the split between the radiation and convection modes of heat transfer is usually unknown. When radiation is used as the mode of calibrating a heat flux gage, it is usually assumed that convection will cause an identical response from the sensor. To check this assumption, the same gage that was calibrated at the AEDC radiation facility was also calibrated in a convection apparatus at Virginia Tech [9]. The convective heat transfer sensitivity of this gage was found to be  $2.33 \mu\text{V}/(\text{W}/\text{cm}^2)$  with a standard deviation of  $0.05 \mu\text{V}/(\text{W}/\text{cm}^2)$ . This represents a 40% higher sensitivity. Although the Gardon gage used in the Virginia Tech tests was separately calibrated in convection by Diller and Borell [11], there is no NIST traceable standard for convection heat transfer. This is an important issue to resolve in future research.

## HIGH-TEMPERATURE FLAME TESTING

Previous oxyacetylene flame tests were conducted with a platinum RTS protected by a layer of aluminum oxide and silicon nitride [9]. These experiments were continued until failure at approximately  $800^{\circ}\text{C}$ . The latest oxyacetylene flame tests reported here were performed with

several complete Platinum/Platinum-10% Rhodium heat flux gages. The final test for each gage was to destruction to determine the temperature limits of the gage.

The gages deposited on aluminum nitride substrates were mounted in a water-cooled aluminum block to provide a heat sink. The block was positioned at a distance of 15 cm (6 in.) from a standard oxyacetylene torch nozzle, as illustrated in Fig. 7. A wide range of flame adjustments was used to create different temperature and heat flux conditions. Tests were performed with different durations and cooling water flow rates. Fig. 8 shows a typical plot of the measured heat flux as recorded in an accompanying videotape. This test is for a relatively short duration and a low heat flux ( $< 100 \text{ W/cm}^2$ ). The final test in this series was performed by turning off all cooling water and proceeding until failure occurred at approximately  $750^\circ\text{C}$ . Other tests performed at much higher heat fluxes produced failure at approximately  $600^\circ\text{C}$ . The sensitivity of the gages had to be estimated by extrapolating the sensitivity versus temperature curve found from the AEDC radiation calibrations to the measured gage surface temperatures. Because this calibration uncertainty introduces considerable uncertainty into the measurements, facilities for performing heat flux calibrations at elevated temperatures are going to be essential.

### LIQUID NITROGEN QUENCH TEST

A liquid nitrogen quenching experiment was performed to test the thermal shock resistance of the Heat Flux Microsensors. The test was done on an RTS to evaluate the adhesion effects of the thin films when exposed to a temperature shock. Adhesion loss of the thin films has been attributed to differences in the thermal expansion coefficients of adjacent films.

An aluminum nitride disk with an RTS deposited on it was heated to  $580^\circ\text{C}$  in a tube furnace. The disk was removed from the furnace and held in air for 25 seconds. The disk was then placed in the liquid nitrogen with the face of the disk submerged for 25 seconds. Finally the disk was entirely submerged in the liquid nitrogen. These three distinct environments can be seen in Fig. 9, with increasing cooling rates for each subsequent section. The air provided a cooling rate of  $2.4^\circ\text{C/sec}$ . With the disk partially submerged the cooling rate increased to  $4.1^\circ\text{C/sec}$ . While the disk was completely submerged the cooling rate increased to  $5.3^\circ\text{C/sec}$ . This produced very vigorous boiling. The thin-film survived without any detectable damage. Future experiments will include liquid nitrogen tests on a complete gage to demonstrate the ability of the microsensors to measure high negative heat fluxes.

### CONCLUSIONS

High temperature Heat Flux Microsensors have been shown to operate well in several severe environments, typical of the aerodynamic testing conditions now being required of instruments. Radiation calibrations demonstrated good response and repeatability of the sensors.

It has also become clear that high temperature heat flux calibration facilities are needed and that comparison between radiation and convection heat transfer under these conditions is needed.

### ACKNOWLEDGEMENTS

The support of the Air Force in this work is acknowledged. The cooperation and encouragement of Carl Kidd while using the facilities at AEDC is greatly appreciated. The authors also acknowledge the cooperation of the Hybrid Microelectronics Laboratory at Virginia Polytechnic Institute and State University.

### REFERENCES

1. Neumann, R. D., "Aerothermodynamic Instrumentation," in **AGARD Report**, No. 761, 1989.
2. Clayton, W. A., "High Temperature Circular Foil Heat-Flux Gage," Hy-Cal Engineering Report TR-417, Feb. 1980.
3. Kidd, C. T., "A Durable, Intermediate Temperature, Direct Reading Heat-Flux Transducer for Measurements in Continuous Wind Tunnels," AEDC-TR-19-81, Nov. 1981.
4. Kidd, C. T., "Recent Developments in High Heat-Flux Measurement Techniques at the AEDC," ISA Paper No. 90-156, 1990.
5. Jones, T. V., "Heat Transfer, Skin Friction, Total Temperature, and Concentration Measurements," in **Measurement of Unsteady Fluid Dynamic Phenomena**, Hemisphere Pub. Corp., N. Y., 1977, pp.63-102.
6. Neumann, R. D., Erbland, P. J., and Kretz, L. D., "Instrumentation of Hypersonic Structures -- A Review of Past Applications and Needs for the Future," AIAA Paper No. 88-2612, 1988.
7. Hager, J. M., Onishi, S., Langley, L. W., and Diller, T. E., "Heat Flux Microsensors," in **Heat Transfer Measurements, Analysis and Flow Visualization**, Ed. R. K. Shah, ASME, 1989, pp. 1-8.
8. Hager, J. M., Simmons, S., Smith, D., Onishi, S., Langley, L. W., and Diller, T. E., "Experimental Performance of a Heat Flux Microsensor," **ASME Journal of Engineering for Gas Turbines and Power**, Vol. 113, 1991, pp. 246-250.

9. Hager, J. M., Terrell, J. P., Langley, L. W., Onishi, S., and Diller, T. E., "Measurements with the Heat Flux Microsensor," Proceedings of the 37th International Instrumentation Symposium, ISA, Research Triangle Park, 1991, pp. 551-561.
10. Kidd, C. T., "Determination of the Uncertainty of Experimental Heat-Flux Calibrations," AEDC-TR-83-13, August 1983.
11. Borell, G. J., and Diller, T. E., "A Convection Calibration Method for Local Heat Flux Gages," ASME Journal of Heat Transfer, Vol. 109, 1987, pp. 83-89.

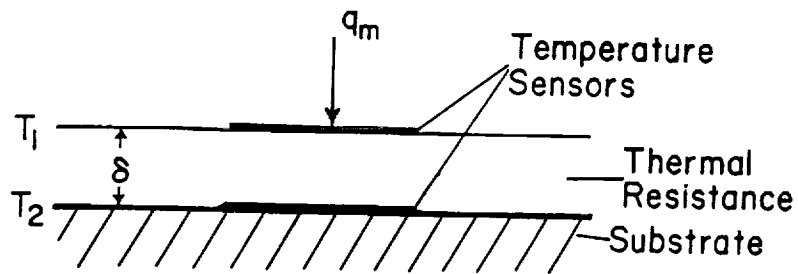


Fig. 1 Layered Heat Flux Gage

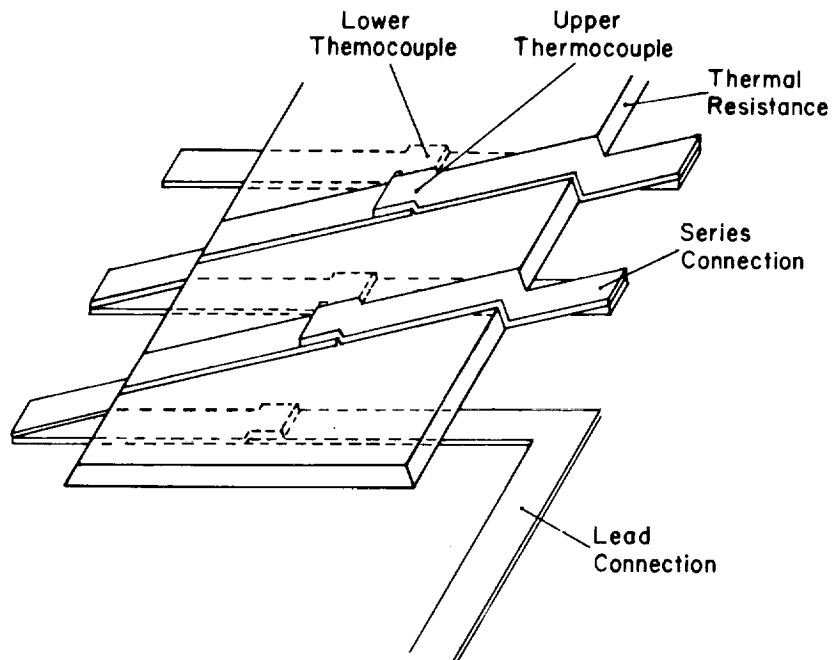


Fig. 2 Detailed Representation of Microsensor

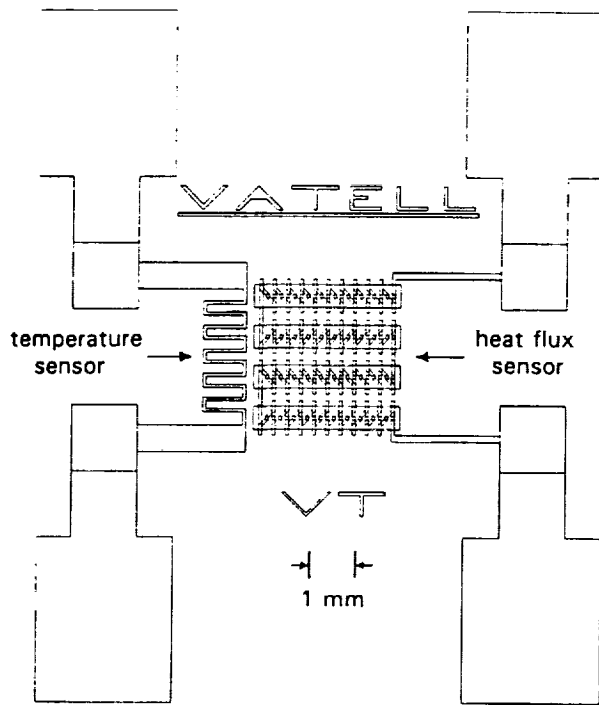


Fig. 3 Heat Flux Microsensor Pattern Overlay

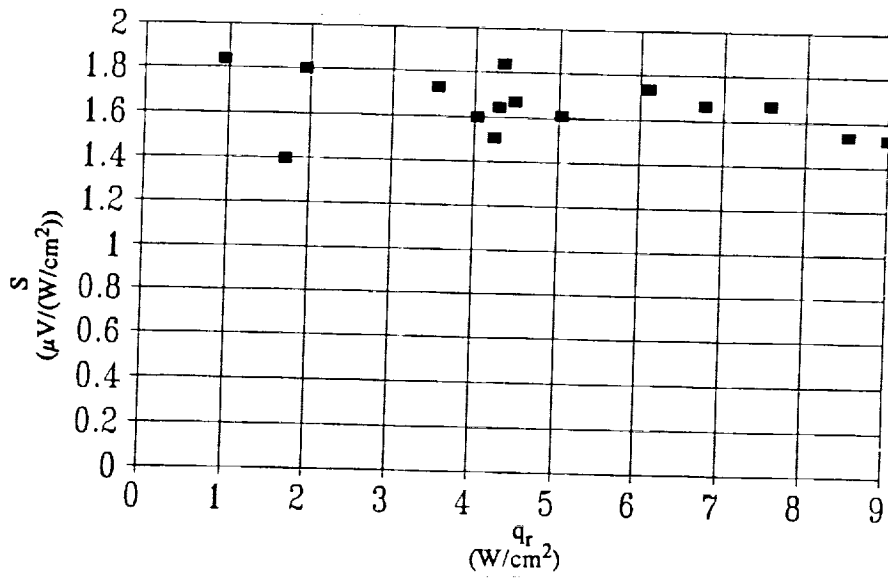


Fig. 4 Low Heat Flux Calibration Tests, Sensitivity Vs. Heat Flux

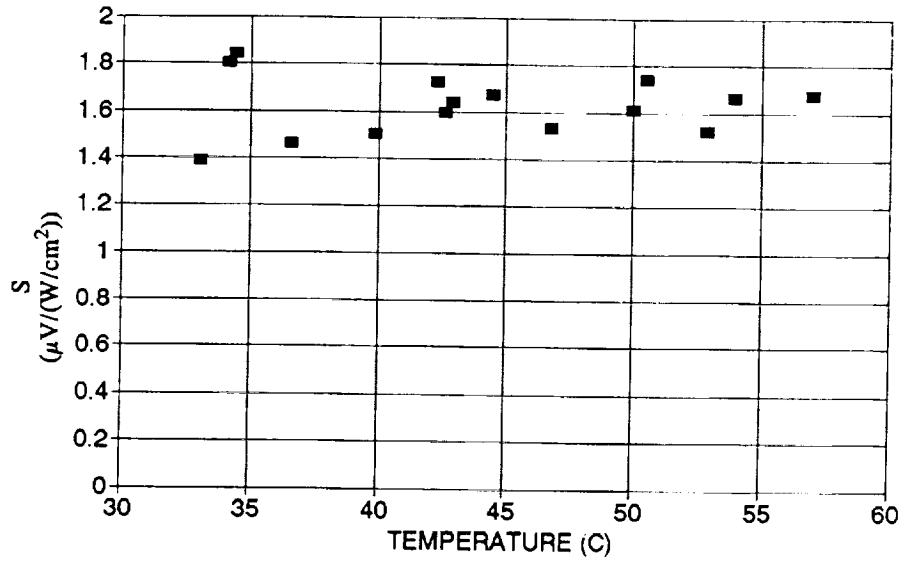
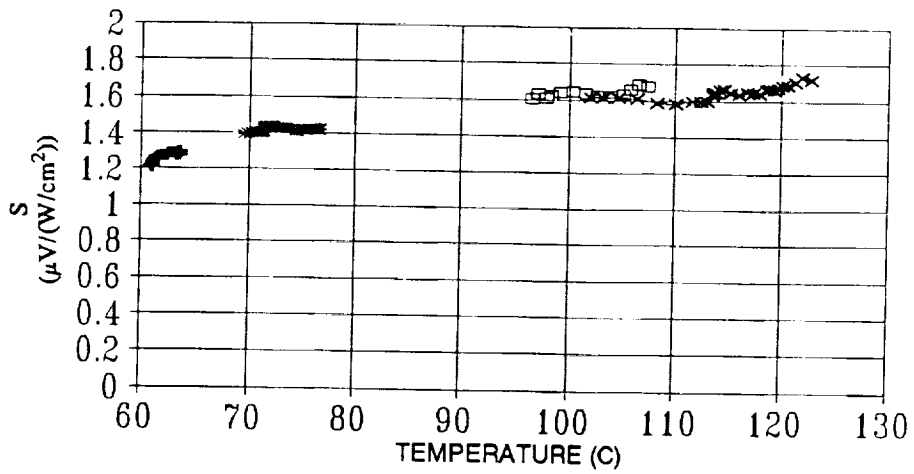


Fig. 5 Low Heat Flux Calibration Tests, Sensitivity Vs. Surface Temperature



+ 201.7 W/cm<sup>2</sup> \* 471.7 W/cm<sup>2</sup> □ 621.9 W/cm<sup>2</sup> -x- 703.5 W/cm<sup>2</sup>

Fig. 6 High Heat Flux Calibration Tests

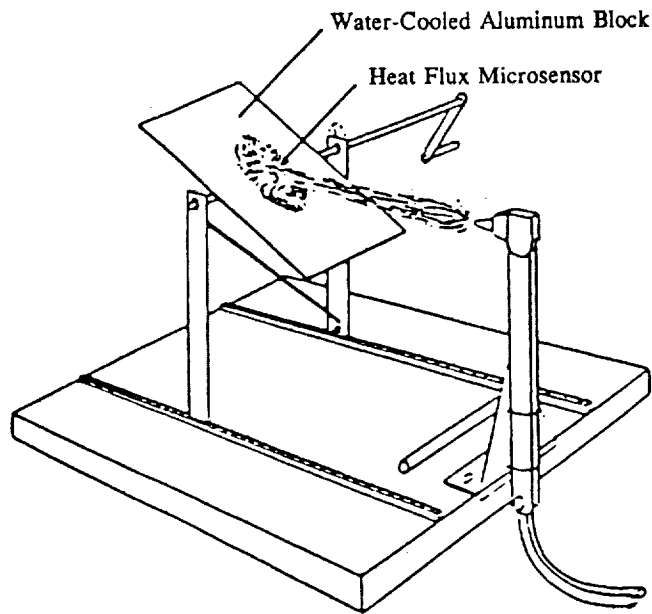


Fig. 7 Oxyacetylene Flame Test Apparatus

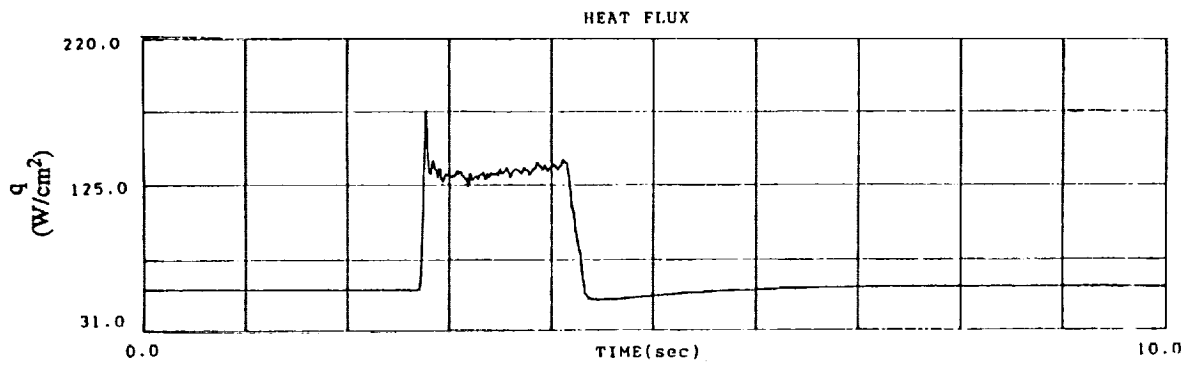


Fig. 8 Sample Oxyacetylene Flame Test

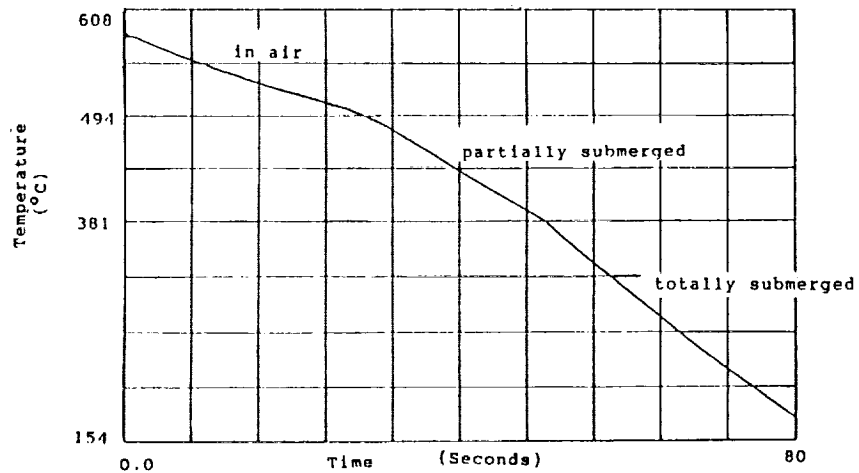


Fig. 9 Liquid Nitrogen Quench Test